High performance polyoxometalate-based cathode materials for rechargeable lithium ion batteries

By Jia-Jia Chen,[1,2] Mark D. Symes,[2] Shao-Cong Fan,[1] Ming-Sen Zheng,[1] Haralampos N. Miras,[2] Quan-Feng Dong,[1*] and Leroy Cronin[2*]

[*] J.-J. Chen, M. D. Symes, S.-C. Fan, M.-S. Zheng, H. N. Miras, Q-F. Dong and L. Cronin
[1]*State Key Laboratory of Physical Chemistry of Solid Surfaces, Collaborative Innovation Centre of Chemistry for Energy Materials, Department of Chemistry, College of Chemistry and Chemical Engineering, Xiamen University, Xiamen, Fujian, 361005, China.*
[2]*WestCHEM, School of Chemistry, the University of Glasgow, University Avenue, Glasgow, G12 8QQ, UK.*

Keywords: Polyoxometalates · Li-ion battery · Cathode material · Electrochemistry

Rechargeable lithium batteries show great promise for high-density energy storage for applications ranging from consumer electronics to electric vehicles and grid balancing.[1] Cathode materials in these batteries are typically oxides of transition metals, which undergo oxidation to higher valences when lithium is removed.[2] Current cathode materials for rechargeable Li-ion batteries are still mainly based on bulk transition metal oxides:[3] distorted rock-salt ±-$NaFeO_2$ structures,[4] spinel structures[5] and olivine structures.[6] However, either the low Li ion mobility and/or the low electronic conductivity of these compounds hamper a high power density output, unless particle sizes are reduced to the nano-scale[7] or carbon coating/doping strategies are employed.[8] In order to satify the increasing demand for high power density and energy density, new cathode materials capable of multi-electron redox reactions and that enable more rapid Li ion transportation (whilst still displaying stable cycling performance) are required.[9]

Recently, polyoxometalates[10] and metal–organic frameworks (MOFs)[11] have been shown to have potential as the cathode materials for rechargeable batteries. For example,

$[Fe^{III}(OH)_{0.8}F_{0.2}(O_2CC_6H_4CO_2)]\cdot H_2O$ (MIL-53(Fe)·H_2O) has been used as the cathode material for Li-based batteries, although the capacity was limited by the low number of electrons (no more than 1 electron per formula unit) involved in the reversible redox reaction.[12] Polyoxometalates are promising multifunctional materials which have numerous applications in catalysis, photoluminescence, as single molecule magnets, and as proton-conductive materials.[13] One of the most important features of POMs is the ability to configure or tailor their redox properties, which allows the development of new functional systems, such as metal–oxide–semiconductor (MOS) flash memory devices[14] and mediators for electrochemical water splitting.[15]

Polyoxometalates have already demonstrated some promise as the cathode in lithium batteries,[10] for example where the active cathode material was phosphomolybdate ($[PMo_{12}O_{40}]^{3-}$) and the anode was lithium metal.[10a] *In-operando* Mo K-edge XAFS measurements on these cathodes revealed that $[PMo_{12}O_{40}]^{3-}$ functioned as an 'electron sponge', cycling reversibly by 24 electrons between $[PMo_{12}O_{40}]^{3-}$ and $[PMo_{12}O_{40}]^{27-}$ during charging/discharging.[16] However, the energy density and power density metrics of these cathode materials was limited by the slow rate of charge/discharge: capacities in excess of 200 mAh g^{-1} could be obtained after 10 cycles, but only at a low current of 1 mA.

In view of this prior art, we hypothesised that vanadium-based polyoxometalates would make excellent cathode material candidates, exhibiting high capacities and rapid charging/discharging whilst also providing a larger operating voltage than the polyoxometalates previously explored for this purpose. Herein, we show that the polyoxovanadate $Li_7[V_{15}O_{36}(CO_3)]$ has multi-electron redox properties suitable for producing cathode materials with a specific capacity of 250 mAh g^{-1}, and energy and power densities of 1.5 kWh L^{-1} and 55 kW L^{-1} respectively in Li-based batteries.

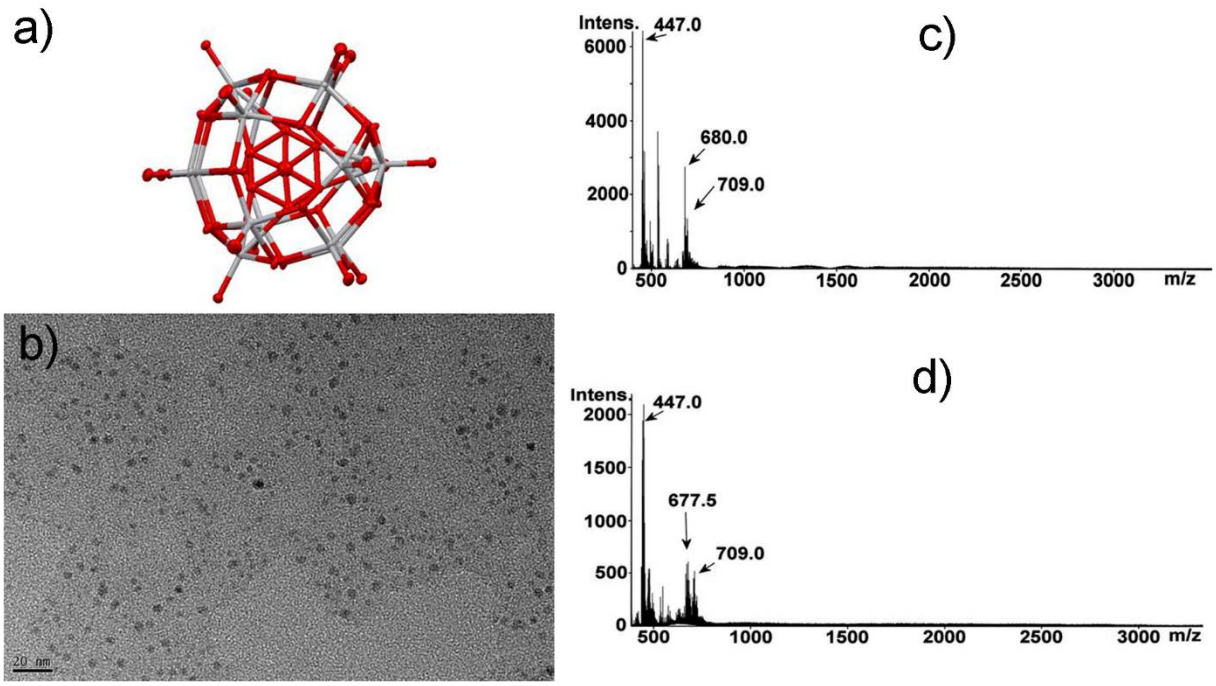

Figure 1 a) The crystal structure of $Li_7[V_{15}O_{36}(CO_3)]$, Gray: vanadium, Red: oxygen. b) TEM image of dehydrated nanoparticles of $Li_7[V_{15}O_{36}(CO_3)]$ after dispersion on a carbon formvar grid (see Supporting Information for preparation details). c) and d) Representation of the negative mode ESI-MS spectra[17a,17b] of $Li_7[V_{15}O_{36}(CO_3)]$ in H_2O:CH_3CN (85:15): **c**: Freshly prepared and dried $Li_7[V_{15}O_{36}(CO_3)]$; **d**: After treatment of $Li_7[V_{15}O_{36}(CO_3)]$ at 200 °C. The data shows that both samples give the same main ion peaks and undergo fragmentation to the same extent.

$Li_7[V_{15}O_{36}(CO_3)]$ was prepared according to an adapted literature procedure[17c] and its crystal structure is shown in Figure 1a. The spherical anion $\{V_{15}O_{36}\}$ of $Li_7[V_{15}O_{36}(CO_3)]$ has a "hollow spheres" structure with an encapsulated CO_3^{2-} group, which has the high crystallographic symmetry D_{3h}, formed by linkage of 15 tetragonal VO_5 pyramids. The 15 V atoms are arranged on the surface of a sphere at a distance of 343 ± 10 pm from the center of the cluster. $\{V_{15}O_{36}\}$ formally contains eight V^{IV} centers and seven V^{V} centers. Six VO_5 pyramids are each linked via three edges and two corners, six further are each linked via two edges and three corners and three are each linked via two edges and four corners. All μ_3-O atoms concomitantly participate in two edge linkages and one corner-linkage; the μ_2-O atoms

form a corner linkage. Such linkages lead to the formation of cubic cages with a cluster anion at each corner, which is further arranged along the three channels occupied by water and cations (See Figure S1). These polyoxovanadate clusters also show good thermal stability when dried at 200 °C under vacuum overnight (Figure S2). As shown in the HRTEM image of Figure 1b, the dehydrated polyoxovanadate clusters form ultra-fine particles less than 5 nm in diameter, probably therefore consisting of some tens of individual polyoxovanadate clusters. Mass spectroscopy of the $\{V_{15}O_{36}\}$ clusters before and after this high temperature treatment confirms that the structure of the $\{V_{15}O_{36}\}$ clusters is retained after heating (*i.e.* they do not coalesce to form bulk oxide), which is also consistent with the results of FTIR (see Figures S3 and S4).

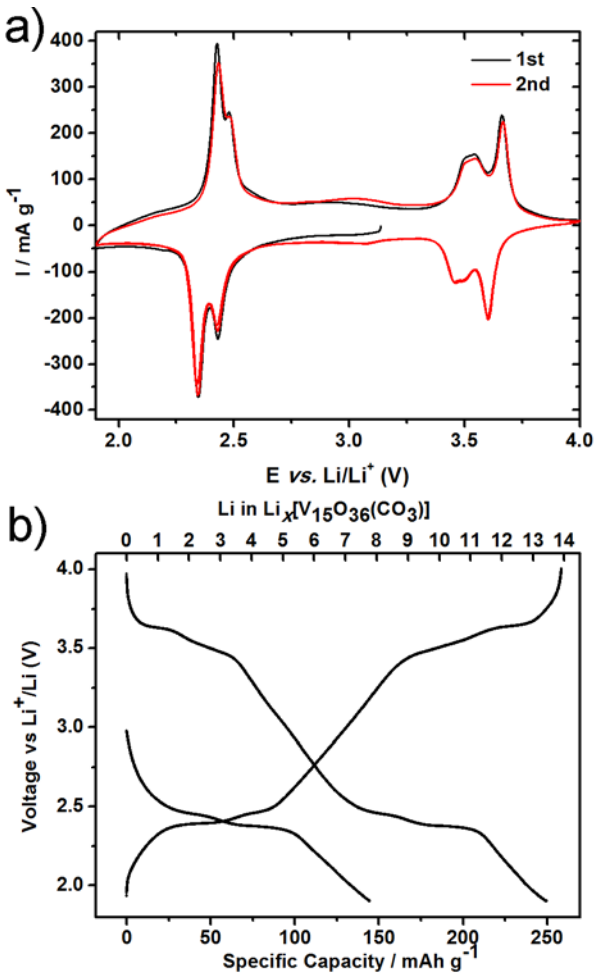

Figure 2 a) CV of the $Li_7[V_{15}O_{36}(CO_3)]$-based cathode at a scan rate of 0.2 mV s^{-1}, starting from open circuit voltage and scanning to low potential (1.9 V), before scanning back to high potential (4.0 V). b) The 1st discharge and 2nd galvanostatic charge-discharge curves of $Li_7[V_{15}O_{36}(CO_3)]$ at a current density of 50 mA g^{-1} over the range 1.9 - 4.0 V.

Interestingly, $Li_7[V_{15}O_{36}(CO_3)]$ shows reversible redox behaviour over the large voltage window 4.0 - 1.9 V *vs.* Li/Li^+, when used in a half-cell with a metallic Li anode with 1 M $LiPF_6$ in ethylene carbonate (EC) + dimethyl carbonate (DMC) + ethyl methyl carbonate (EMC) (1:1:1, v/v) as the electrolyte. As illustrated by the cyclic voltammetry (Figure 2a), the polarization ”E between the reduction and oxidization processes is small and the CVs of the first and second sweeps overlay well, indicating functional stability for the cathode and suggesting that $Li_7[V_{15}O_{36}(CO_3)]$ does not decompose during cycling. Meanwhile, the redox peaks are distributed in two voltage zones: 2.2 – 2.6 V and 3.3 – 3.7 V. In order to understand the cycling behaviour of $Li_7[V_{15}O_{36}(CO_3)]$, galvanostatic charging-discharging was carried out to calculate the number of Li^+ ions translocating during these redox processes. As shown in the galvanostatic charging-discharging profiles in Figure 2b, $Li_7[V_{15}O_{36}(CO_3)]$ delivers an initial discharging capacity of 140 mAh g^{-1} at a current density of 50 mA g^{-1}. When charging back to 4.0 V *vs.* Li^+/Li, a reversible charging-discharging capacity of 250 mAh g^{-1} is obtained for these $\{V_{15}O_{36}\}$ clusters. According to the equation:

$$Q = (nF)/(3.6M_w) = (96500n)/(3.6\ M_w),$$

where Q is the reversible charging-discharging capacity, n is the number of electrons passed during the redox reaction and M_w is the molecular weight of $Li_7[V_{15}O_{36}(CO_3)]$ (M_w =1448.7 g mol^{-1}), the translocation of each Li^+ to/from the polyoxovanadate cluster contributes a capacity of around 18.5 mAh g^{-1}. As a result, we calculate that between seven and eight V^V centers (140/18.5) are electrochemically reduced to V^{IV} during the 1st discharging process,

and that 13.5 V^{V} centers (250/18.5) undergo electrochemical oxidization during the subsequent charging process (and in the charge-discharge processes thereafter). The theoretical specific capacity for $Li_x[V_{15}O_{36}(CO_3)]$ within this voltage window can then be calculated by taking n to be 14 (the next nearest integer number of electrons), and feeding this number back into the equation above to find a theoretical specific capacity for $Li_x[V_{15}O_{36}(CO_3)]$ of 259 mAh g^{-1}.

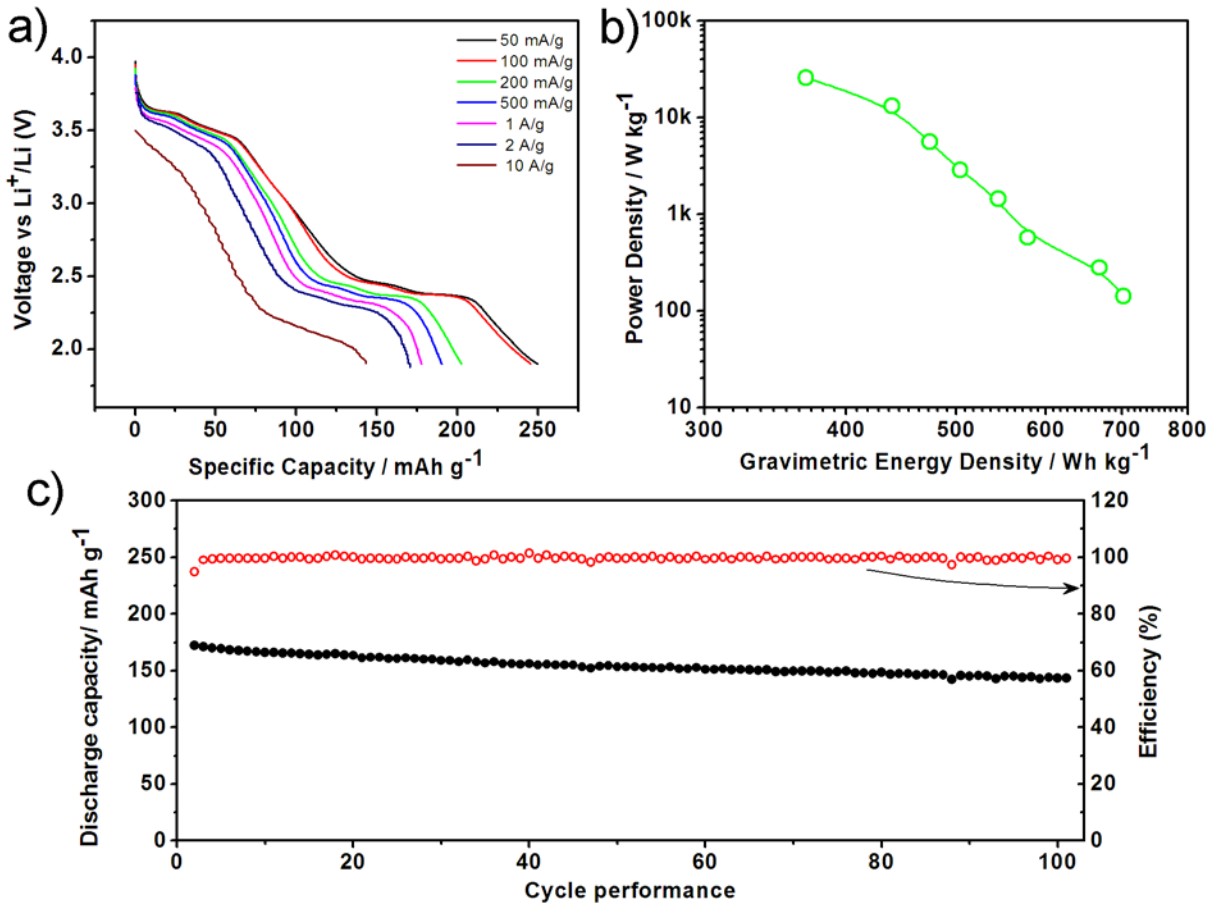

Figure 3 a) Discharge curves for $Li_7[V_{15}O_{36}(CO_3)]$ over the voltage range of 1.9 - 4.0 V *vs*. Li^+/Li at different current densities; b) Ragone plot comparing the power and gravimetric energy densities based on the mass of $Li_7[V_{15}O_{36}(CO_3)]$. c) Cycle performance with coulombic efficiency of $Li_7[V_{15}O_{36}(CO_3)]$ at the high current densiy of 2 A g^{-1} over 100 cycles.

$Li_7[V_{15}O_{36}(CO_3)]$ shows high rates performance when tested as a cathode over the voltage range 1.9 - 4.0 V (Figure 3a). The polarization of the discharging plateaus is not great when

subjected to a high charging-discharging current density, and 170 mAh g^{-1} can be obtained at a high discharge rate of 2 A g^{-1}, and a specific capacity of around 140 mAh g^{-1} is possible at the even more extreme current density of 10 A g^{-1}. This excellent rates and cycling performance at high current density (with almost 100% coulombic efficiency over 100 cycles, Figure 3c) could be due to the ultra-fine size of the $Li_7[V_{15}O_{36}(CO_3)]$ active material (Figure 1b), and ensures a high power density output of 25.7 kW kg^{-1} with an energy density output of 370 Wh kg^{-1} (Figure 3b). In terms of volumetric densities (and taking the crystal density of $Li_7[V_{15}O_{36}(CO_3)]$ to be 2.15 g cm^{-3}), $Li_7[V_{15}O_{36}(CO_3)]$ exhibits energy and power densities of 1.5 kWh L^{-1} and 55 kW L^{-1}.

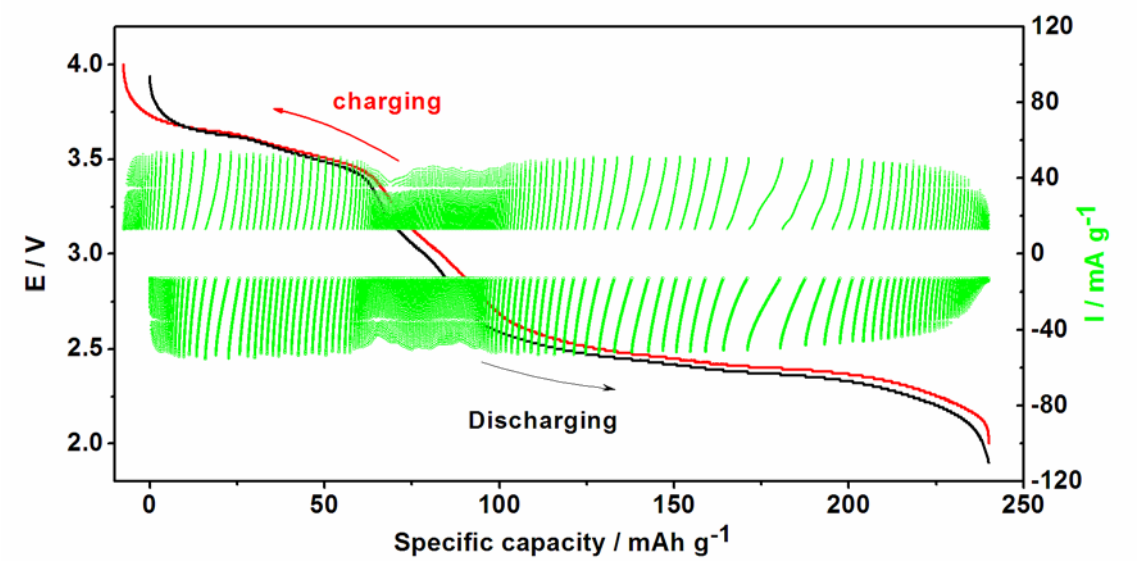

Figure 4. The chronoamperometric response of the $Li_7[V_{15}O_{36}(CO_3)]$-based electrode by the potentiostatic intermittent titration techniques method (PITT). An expansion of the zone between 50-120 mAh g^{-1} can be found in the Supporting information (Figure S5).

The kinetics of the various reversible redox processes of $Li_7[V_{15}O_{36}(CO_3)]$ were studied by the potentiostatic intermittent titration techniques (PITT) method.[12,18] As shown in Figure 4, the chronoamperometric response of $Li_7[V_{15}O_{36}(CO_3)]$ indicated no obvious bell-shape variation, suggesting that Li ion migration is not kinetically limited by a two-phase interface in these electrodes. In fact, all the current curves decay gradually during each potential step

and almost follow a Cottrell-type law, indicative of a solid solution insertion process kinetically limited by Li^+ diffusion. This behaviour is significantly different from the intercalation processes found in the bulk oxides commonly used in Li-ion batteries, such as the $LiMPO_4$[19] and $Li_xV_2O_5$ systems.[20] $Li_xV_2O_5$ generally displays 4 or 5 plateau regions, each one corresponding to a two-phase process, while $Li_7[V_{15}O_{36}(CO_3)]$ has similar redox behaviour but corresponding to a solid solution insertion process. As a result, a methodology based on galvanostatic intermittent titration techniques (GITT) and electrochemical impedance spectroscopy (EIS) [21] can be used to estimate the apparent chemical diffusion coefficient of Li^+ in the $Li_7[V_{15}O_{36}(CO_3)]$-based cathode. As shown in Figure S6, the $D_{aap,Li}$ values are comparatively high over the voltage range 2.2 - 3.9 V, with values ranging from 1.4×10^{-10} to 2.3×10^{-7} $cm^2\ s^{-1}$, showing that the mobility of Li^+ ions remains high in this material when compared to other bulk metal oxides such as $LiCoO_2$ (10^{-12} to 10^{-10} $cm^2\ s^{-1}$ over the voltage range 3.85 – 4.35 V)[22] and V_2O_5 (10^{-11} to 10^{-8} $cm^2\ s^{-1}$ over the voltage range 3.2 – 3.45 V).[23] The progressively decreasing concentration of vacant sites available for Li^+ as intercalation of Li^+ proceeds would cause a lower diffusion coefficient in $LiCoO_2$,[24] while the variation of diffusion coefficient with voltage in $Li_7[V_{15}O_{36}(CO_3)]$ suggests a decreasing number of uptake/removal sites for Li^+ on the surface of the cluster. $Li_7[V_{15}O_{36}(CO_3)]$ is an open-framework material consisting of multiple individual polyoxovanadate clusters, each of which has multiple vanadium centers undergoing redox cycling, and as such it may have a rather different Li-ion transportation mechanism to that displayed in traditional bulk metal oxide cathodes. The rapid diffusion of Li^+ in the $Li_7[V_{15}O_{36}(CO_3)]$-based cathodes suggests that the uptake/removal processes of Li ions in polyoxometalate-based batteries are somewhat easier than the intercalation/de-intercalation processes at work in bulk metal oxides. Moreover, the electronic conductivity of the $Li_7[V_{15}O_{36}(CO_3)]$ cathode material was found to be 1.12×10^{-6} S cm^{-1} at 20 °C (Figure S7), which also compares favourably with

currently available cathode materials (around 1×10^{-9} S cm^{-1} for $LiFePO_4$ and around 1×10^{-6} S cm^{-1} for $LiCoO_2$). We note that Mizuno and co-workers have recently studied the cooperative migration of electrons and alkali metal ions in porous ionic crystals based on polyoxometalates in some detail, which may be relevant to this discussion.[25]

Control experiments using equivalent loadings of $LiVO_3$ and V_2O_5 (two likely decomposition products of $Li_7[V_{15}O_{36}(CO_3)]$) showed that these simpler oxides of vanadium exhibit impaired and/or less stable behaviour than $Li_7[V_{15}O_{36}(CO_3)]$ when used as the base materials for Li battery cathodes (see Figures S8 and S9). Considering the reversibility of the charge-discharge processes of the $Li_7[V_{15}O_{36}(CO_3)]$-based electrodes, it thus seems likely that higher nuclearity polyoxometalate clusters are required in order to achieve the activity observed in the batteries studied herein. These control experiments also suggest that decomposition of the polyoxometalate clusters to these simpler oxides does not occur to a significant degree over the number of cycles studied. In a similar way, cathodes containing $Li_7[V_{15}O_{36}(CO_3)]$ that had been cycled in a battery 10 times were extracted with water, and mass spectrometry was performed on the material dissolved out of these electrodes. This data (see Figure S10) shows that the molecular polyoxometalate cluster is still present in the cathode after multiple cycling events.

In conclusion, our studies of $Li_7[V_{15}O_{36}(CO_3)]$ have identified polyoxovanadates as a new class of potential cathode material for future high energy and power density Li ion rechargeable batteries. Rapid lithium ion diffusion and good electron conductivity in $Li_7[V_{15}O_{36}(CO_3)]$ should allow rapid charging and discharging of the resulting battery, and we have shown that a power density output of 25.7 kW kg^{-1} (55 kW L^{-1}) is possible with this material. In contrast to the bulk oxides traditionally used as cathode and anode materials in rechargeable batteries, the polyoxometalate investigated herein can undergo multi-electron reduction whilst still retaining its cluster structure. On account of the wealth of readily-

accessed polyoxometalate structures, we believe that this approach will provide great opportunity to optimize different functional materials to fulfill various electrochemical applications.

Experimental

Synthesis of $Li_7[V_{15}O_{36}(CO_3)]$ and Characterization. $Li_7[V_{15}O_{36}(CO_3)]$ was prepared according to an adapted literature procedure.[17c] TGA-DTA was carried out on a Pyris Diamond TG-DTA (PE Co., US) to obtain the optimized treatment temperature in a constant flow of dry N_2 (50 ml min^{-1}) and a heating/cooling rate of 10 °C min^{-1}. Alumina crucibles were loaded with 5-10 mg of sample powder. The weight loss before 200 °C (see Figure S2) is ascribed to the dehydration of $Li_7[V_{15}O_{36}(CO_3)]\cdot nH_2O$. The optimized treatment temperature was determined to be 200 °C and the samples were placed into a furnace to anneal at 200 °C for 10 h under N_2, and then were pulverized to a fine powder by ball milling after cooling to room temperature. The purity of the as-prepared and dehydrated samples was characterized by IR spectroscopy. The morphology of the dehydrated $Li_7[V_{15}O_{36}(CO_3)]$ powder was observed by field-emission scanning electron microscopy (SEM Hitachi S-4800) and transmission electron microscopy (TEM Hitachi JEM-2100, 200 KV). The structural stability of $Li_7[V_{15}O_{36}(CO_3)]$ was also investigated by mass spectroscopy which was collected using a Q-trap, time-of-flight MS (MicrOTOF-Q MS) instrument supplied by Bruker Daltonics Ltd. The detector was a time-of-flight, micro-channel plate detector and all data was processed using the Bruker Daltonics Data Analysis 3.4 software, whilst simulated isotope patterns were investigated using Bruker Isotope Pattern software and Molecular Weight Calculator 6.45. The calibration solution used was Agilent ES tuning mix solution, Recorder No. G2421A, enabling calibration between approximately 100 m/z and 3000 m/z. This solution was diluted 60:1 with MeCN. Samples were introduced into the MS *via* direct

injection at 180 μL/h. The ion polarity for all MS scans recorded was negative at 180 ^{o}C, with the voltage of the capillary tip set at 4000 V, collision cell RF 1250 Vpp, transfer time 90 μs, end plate offset at –500 V, funnel 1 RF at 300 Vpp and funnel 2 RF at 400 Vpp.

Electrochemical testing. $Li_7[V_{15}O_{36}(CO_3)]$ crystals were placed into a furnace to anneal at 200 °C for 6 h under N_2, and then were pulverized to a fine powder by ball milling after cooling to room temperature. The cathodes were then prepared by mixing 70 wt% $Li_7[V_{15}O_{36}(CO_3)]$, 20 wt% acetylene black and 10 wt% PVDF binder. The resulting slurries were coated onto Al foil current collectors by a doctor blade method and dried at 105 °C under vacuum overnight. Such a cathode, a lithium foil anode, a Cellgard2400 separator and the electrolyte were then sealed into a CR2016-type coin cell. 1 M $LiPF_6$/ethylene carbonate (EC) + dimethyl carbonate (DMC) + ethyl methyl carbonate (EMC) (1:1:1, v/v) was used as the electrolyte. Cyclic voltammetry measurements were carried out over the voltage range 1.9 - 4.0 V at a scan rate of 0.2 mV s^{-1} using a multi-channel potentiostat (VMP2, Bio-logic Instruments). The galvanostatic charge–discharge testing was conducted on a NEWARE BTS-5V/5mA type battery charger (Shenzhen NEWARE Co., China) over the voltage range 1.9 - 4.0 V. All the cathodes used had mass loadings of around 1.2 mg cm^{-2}.

A detailed description of the conductivity testing, the cation insertion process and the determination of the diffusion coefficient can be found in the Supporting Information.

Supporting information

Supporting information for this article is available on Wiley InterScience or from the author.

Acknowledgements

We gratefully acknowledge financial support from National 973 Program (2015CB251102), the NSFC Key Project (U1305246, 21321062) and the NFFTBS (No. J1310024). We thank

Dr. De-Liang Long (University of Glasgow) for useful discussions. MDS thanks the University of Glasgow for a Kelvin-Smith Research Fellowship and LC thanks the Royal Society for a Wolfson merit award.

Received: ((will be filled in by the editorial staff))
Revised: ((will be filled in by the editorial staff))
Published online: ((will be filled in by the editorial staff))

[1] M. S. Whittingham, *Chem. Rev.* **2004**, *104*, 4271.

[2] a) J. W. Fergus, *J. Power Sources* **2010**, *195*, 939; b) B. Scrosati, J. Garche, *J. Power Sources* **2010**, *195*, 2419.

[3] V. Etacheri, R. Marom, R. Elazari, G. Salitra, D. Aurbach, *Energy Environ. Sci.* **2011**, *4*, 3243.

[4] a) H. Chen, C. P. Grey, *Adv. Mater.* **2008**, *20*, 2206; b) K. M. Shaju, P. G. Bruce, *Adv. Mater.* **2006**, *18*, 2330.

[5] a) S. Lee, Y. Cho, H.-K. Song, K. T. Lee, J. Cho, *Angew. Chem., Int. Ed.* **2012**, *51*, 8748; b) D. K. Kim, P. Muralidharan, H.-W. Lee, R. Ruffo, Y. Yang, C. K. Chan, H. Peng, R. A. Huggins, Y. Cui, *Nano Lett.* **2008**, *8*, 3948.

[6] a) C. Delmas, M. Maccario, L. Croguennec, F. Le Cras, F. Weill, *Nat. Mater.* **2008**, *7*, 665; b) A. K. Padhi, K. S. Nanjundaswamy, J. B. Goodenough, *J. Electrochem. Soc.* **1997**, *144*, 1188; c) J. M. Clark, S.-i. Nishimura, A. Yamada, M. S. Islam, *Angew. Chem., Int. Ed.* **2012**, *51*, 13149.

[7] a) B. Kang, G. Ceder, *Nature* **2009**, *458*, 190; b) Y. Wang, G. Cao, *Adv. Mater.* **2008**, *20*, 2251.

[8] B. Lung-Hao Hu, F.-Y. Wu, C.-T. Lin, A. N. Khlobystov, L.-J. Li, *Nat. Commun.* **2013**, *4*, 1687.

[9] a) X. P. Gao, H. X. Yang, *Energy Environ. Sci.* **2010**, *3*, 174; b) M. S. Islam, C. A. J. Fisher, *Chem. Soc. Rev.* **2014**, *43*, 185.

[10] a) N. Kawasaki, H. Wang, R. Nakanishi, S. Hamanaka, R. Kitaura, H. Shinohara, T. Yokoyama, H. Yoshikawa, K. Awaga, *Angew. Chem., Int. Ed.* **2011**, *50*, 3471; b) H. Yoshikawa, C. Kazama, K. Awaga, M. Satoh, J. Wada, *Chem. Commun.* **2007**, 3169; c) H. Yoshikawa, S. Hamanaka, Y. Miyoshi, Y. Kondo, S. Shigematsu, N. Akutagawa, M. Sato, T. Yokoyama, K. Awaga, *Inorg. Chem.* **2009**, *48*, 9057; d) Y.-G. Chen, C.-G. Wang, X.-Y. Zhang, D.-M. Xie, R.-S. Wang, *Synthetic Met.* **2003**, *135-136*, 225; e) Y. Ji, J. Hu, L. Huang, W. Chen, C. Streb, Y.-F. Song, *Chem. Eur. J.* **2015**, *21*, 6469.

[11] a) Z. Zhang, H. Yoshikawa, K. Awaga, *J. Am. Chem. Soc.* **2014**, *136*, 16112; b) Y. Lin, Q. Zhang, C. Zhao, H. Li, C. Kong, C. Shen, L. Chen, *Chem. Commun.* **2015**, *51*, 697; c) J. Qian, M. Zhou, Y. Cao, X. Ai, H. Yang, *Adv. Energy Mater.* **2012**, *2*, 410.

[12] G. Férey, F. Millange, M. Morcrette, C. Serre, M.-L. Doublet, J.-M. Grenèche, J.-M. Tarascon, *Angew. Chem., Int. Ed.* **2007**, *46*, 3259.

[13] a) H. N. Miras, J. Yan, D.-L. Long, L. Cronin, *Chem. Soc. Rev.* **2012**, *41*, 7403; b) H.-Y. Zang, J.-J. Chen, D.-L. Long, L. Cronin, H. N. Miras, *Adv. Mater.* **2013**, *25*, 6245.

[14] C. Busche, L. Vila-Nadal, J. Yan, H. N. Miras, D.-L. Long, V. P. Georgiev, A. Asenov, R. H. Pedersen, N. Gadegaard, M. M. Mirza, D. J. Paul, J. M. Poblet, L. Cronin, *Nature* **2014**, *515*, 545.

[15] a) B. Rausch, M. D. Symes, G. Chisholm, L. Cronin, *Science* **2014**, *345*, 1326; b) M. D. Symes, L. Cronin, *Nat. Chem.* **2013**, *5*, 403.

[16] a) H. Wang, S. Hamanaka, Y. Nishimoto, S. Irle, T. Yokoyama, H. Yoshikawa, K. Awaga, *J. Am. Chem. Soc.* **2012**, *134*, 4918; b) Y. Nishimoto, D. Yokogawa, H. Yoshikawa, K. Awaga, S. Irle, *J. Am. Chem. Soc.* **2014**, *136*, 9042; c) H. Wang, T. Yamada, S. Hamanaka, H. Yoshikawa, K. Awaga, *Chem. Lett.* **2014**, *43*, 1067; d) H. Yang, T. Song, L. Liu, A. Devadoss, F. Xia, H. Han, H. Park, W. Sigmund, K. Kwon, U. Paik, *J. Phys. Chem. C*, **2013**, *117*, 17376.

[17] a) H. N. Miras, E. F. Wilson, L. Cronin, *Chem. Commun.* **2009**, 1297; b) E. F. Wilson, H. N. Miras, M. H. Rosnes, L. Cronin, *Angew. Chem. Int. Ed.* **2011**, *50*, 3720; c) A. Müller, M. Penk, R. Rohlfing, E. Krickemeyer, J. Döring, *Angew. Chem., Int. Ed. Engl.* **1990**, *29*, 926.

[18] N. Recham, J. N. Chotard, L. Dupont, C. Delacourt, W. Walker, M. Armand, J.-M. Tarascon, *Nat. Mater.* **2010**, *9*, 68.

[19] C. A. J. Fisher, V. M. Hart Prieto, M. S. Islam, *Chem. Mater.* **2008**, *20*, 5907.

[20] X. Rocquefelte, F. Boucher, P. Gressier, G. Ouvrard, *Chem. Mater.* **2003**, *15*, 1812.

[21] W. Weppner, R. A. Huggins, *Annu. Rev. Mater. Sci.* **1978**, *8*, 269.

[22] M. D. Levi, G. Salitra, B. Markovsky, H. Teller, D. Aurbach, U. Heider, L. Heider, *J. Electrochem. Soc.* **1999**, *146*, 1279.

[23] S.-I. Pyun, J.-S. Bae, *Electrochim. Acta* **1996**, *41*, 919.

[24] A. Van der Ven, J. Bhattacharya, A. A. Belak, *Acc. Chem. Res.* **2012**, *46*, 1216.

[25] R. Kawahara, S. Uchida, N. Mizuno, *Chem. Mater.* **2015**, *27*, 2092.